

## Modelling Fluidized Beds using Coupled Discrete Element Modelling with Computational Fluid Dynamics

C. Marie, S. Al Arkawazi, K. Benhabib and P. Coorevits  
Université de Picardie Jules Verne  
Eco-PRocédés, Optimisation et Aide à la Décision, (EPROAD EA-4669)  
IUT de l'Aisne, Saint-Quentin, France

### Abstract

Fluidized bed units are found in many plant operations in chemical reactors, water or air treatment, pharmaceutical, and mineral industries. These multi-physics problems are still insufficiently controlled, leaving the moment a great place to macroscopic and empirical approaches. The aim of the work is to simulate the behavior of fluidized bed, better understand to several characteristic phenomena (such as bubbling, slugging...etc), and at the end, to optimize the process. Discrete Element Method (DEM) on the basis of Newton's laws of motion applied to individual particles and Computational Fluid Dynamics (CFD) on based on the Navier-Stokes equations applied by Salome platform and code\_Saturne for calculation of fluid flow. A model that combines the discrete element method (DEM) and computational fluid dynamics (CFD) was developed. In first step calculate the drag force in three-dimension (3D) fluid flow over one sphere with different diameters (0.5, 1 and 2 mm) which held fixe in the passage of fluid stream, for two types of meshing (moderate and fine) numerically, later The interaction between the fluid and each particle is performed through a drag force, and the effect of local particles concentration on the drag force is modeled by a porosity function  $f(\varepsilon) = \varepsilon^{-n}$ . Numerical results are compared with those obtained using an experimental fluidization device for two cylindrical column internal diameters (97, 42.3 mm) respectively, in terms of heights of the fluidized bed for different fluid velocities. The comparison of numerical simulations with experimental results, (in two columns with different diameters) already presents a very good fit, while the coupling model is relatively simple.

**Keywords:** fluidization, coupling (DEM-CFD), porosity function.

# 1 Introduction

Fluidization is a process in which a gas or liquid is blown upward and evenly through a bed of solid particles with sufficient force to cause the particles to rise up and move around inside their container. The most common reason for fluidizing a bed is to obtain vigorous agitation of the solid particles in contact with the fluid, leading to excellent contact of the solid particles and the fluid and the solid and the wall. Good mixing of the solid which avoids the presence of local hot or cold points in the reactors. For these reasons fluidized bed units are used in a variety of industries such as oil, petrochemicals, minerals, pharmaceutical and food processing. Accurate models which provide detailed information on the key phenomena occurring in the bed are necessary to properly design and operate fluidized beds at the desired conditions. One parameter of particular interest when working with fluidized beds is the minimum fluidization velocity, experiments show that the minimum fluidization velocity of particles increases as the diameter of the fluidization column is reduced, or if the height of the bed is increased. These trends are shown to be due to the influence of the wall[1]. During the past 30 years, there have been continuous and vigorous attempts in the direction of reducing empiricism. In particular, developments in Computational Fluid Dynamics CFD have accelerated in the past two decades because of the spectacular progress in the digital computing. CFD has now emerged as a powerful tool for solving the governing equations of change for laminar and turbulent flows for single as well as multiphase flows. A balanced combination of CFD and experiments gives fairly good knowledge of flow pattern in the equipment under consideration. The macroscopic behavior of particulate matter is controlled by the interactions between individual particles as well as interactions with surrounding gas or liquid and wall. Understanding the microscopic mechanism in terms of these interactions is therefore the key leading to truly interdisciplinary research into particulate matter and producing results that can be generally used. In recent years, such research has been rapidly developed worldwide, mainly as a result of the rapid development of discrete particle simulation technique and computer technology. Several discrete modeling techniques have been developed, Discrete Element Method (DEM) simulations can provide dynamic information[2], such as the trajectories of and transient forces acting on individual particles, which is extremely difficult, if not impossible, to obtain by physical experimentation at this stage of development. Consequently[3, 4], it has been increasingly used in the past two decades or so. Computational models that coupling DEM-CFD have proved effective in reproducing most of the features on both microscopic and macroscopic scales of complex units involving multiphase flows[5, 6], this is particularly true for first principles models, which typically are not directly applicable to the real scale of the plant but can produce realistic data crucial for fundamental studies. According to [7, 8], there are three schemes in the previous DEM-CFD simulation of fluid (gas)-solid flow in fluidization:

Scheme 1: The force from the particles to the gas phase is calculated by a local-average method as used in the Two Fluid Models (TFM), whereas the force from the gas phase to each particle is calculated separately according to individual-particle

velocity[9, 10].

Scheme 2: The force from the particles to the gas phase is calculated first at a local-average scale as used in scheme 1. This value is then distributed to individual particles according to a certain average rule [11, 12].

Scheme 3: At each time step, the particle fluid interaction forces on individual particles in a computational cell are calculated first, and the values are then summed to produce the particle-fluid interaction force at the cell scale [13, 14, 15].

According to the Newton's third law of motion, the force of the solid phase acting on the gas phase should be equal to the force of the gas phase acting on the solid phase but in the opposite direction. Scheme 1 does not guarantee that this condition can always be satisfied. Consequently, it is not reasonable. Indeed, this scheme was used only in the early stage of DEM-CFD development, although it can still be found occasionally. Scheme 2 can satisfy Newton's third law. However, it uniformly distributes the interaction force among the particles in a computational cell irrespective of the different behaviors of these particles in the cell. This scheme cannot fully represent reality, as the particle-fluid interaction forces for the particles in the cell should differ for non uniform particle-fluid flow. In addition, in the calculation of the particle-fluid interaction force, a mean particle velocity has to be used. The appropriate method for calculating this mean particle velocity is still an open question, particularly for multisized particle systems. Scheme 3 can overcome the above problems associated with schemes 1 and 2. Indeed, this scheme has been widely accepted since its first introduction by[11]. In order to predict and study the trajectory of the particulate, it is important to understand the flow structures and how they influence the hydrodynamic forces on the particulate. Significant research effort has been made into studying the flow past a stationary sphere over a wide range of Reynolds numbers both experimentally [16, 17, 18] and numerically [19, 20], in this study the coupling of DEM-CFD is follow Scheme 3 .

The motivations of this study are: 1) coupling DEM-CFD by using a simple model for calculating the interactions between the fluid and particles is performed through a drag force( $F_D$ ) by using Salome-platform and Code\_ Saturne for calculation of fluid flow CFD and code SIGRAME which developed in lab for calculation of DEM on the basis of Newton's laws of motion applied to individual particles in two dimension (2D); 2) calculate the drag force in 3D fluid flow over one stationary sphere fluid with different sizes, using two types of meshing (moderate and fine) numerically, in order to extend the understanding of a sphere's trajectory due to rotation, the flow over a stationary sphere is investigated in the turbulence regime at ( $Re_p = 1000 - 10000$ ) for different diameter spheres(0.5, 1 and 2 mm) ; 3) calculate the drag force for fluidized bed and the effect of local particles concentration on the drag force is modeled by a porosity function  $f(\varepsilon) = \varepsilon^{-n}$  numerically[21]; 4) comparing the numerical results with experimental results obtained from fluidization device for two cylindrical column with internal diameters (97, 42.3 mm) respectively, in terms of heights of the fluidized bed for different fluid velocities.

## 2 Numerical approach

### 2.1 Computational Fluid Dynamics (CFD) approach

The codes used in this research are Salome platform version (5.1.5) and Code\_ Saturne version (1.3.3) which produced by EDF of France are general purpose computational fluid dynamics software. Developed since 1997 by EDF R& D, it is based on a co-located Finite Volume approach that accepts meshes with any type of cell for calculations of the fluid flow. Salome platform is used for design and mesh the geometry of the case, later using code\_ Saturne which is based on the Navier-Stokes equations. Code\_ Saturne produces a file of results in 3D that include the coordinates and velocities for each node , and pressure for each element for the mesh. The general differential formulations of the Navier-Stokes equations for fluid flow are:

Continuity equation (equation or mass balance):

$$\frac{\partial \rho}{\partial t} + \vec{\nabla} \cdot (\rho \vec{v}) = 0 \quad (1)$$

Momentum equation of the quantity of motion:

$$\frac{\partial(\rho \vec{v})}{\partial t} + \vec{\nabla} \cdot (\vec{v} \otimes \vec{v}) = -\vec{\nabla} \cdot p + \vec{\nabla} \tau + \vec{f} \quad (2)$$

Where  $t$  is time,  $\rho$  is density of fluid,  $\vec{v}$  is velocity of fluid,  $p$  is pressure,  $\tau$  is the viscous stress tensor and  $\vec{f}$  refers to the resultant of the forces exerted mass in the fluid. Code\_Saturne gave a file of results in 3D that include the coordinates and velocities for each node in the mesh, and pressure for each element in the mesh.

### 2.2 Particle dynamics

#### 2.2.1 Discrete element modeling of granular media

The most general method of discrete elements is used to model real deformable particles and complex forms (from the ellipsoid to the polygon). We consider here only if "simple" of spherical non-deformable and non-penetrable. Element Method provides discrete coordinates, speed and reactions of contact of each particle at each time step. Modeling discrete element solver used as the contact bipotential initiated by De Saxc [22]. In addition, it uses the concept NSCD (Non Smooth Contact Dynamics) developed by M. Jean and J.J. Moreau, allowing to correctly model the dynamic effects but also to work with a step size large in comparison with explicit codes. The calculation algorithm is a "step by step". For each pair of candidate particles in contact, the variables are put in duality the local relative velocity and the contact reaction. The introduction of Coulomb friction leads to a nonlinear problem that cannot be solved by linear programming method. Unlike the usual approach, the bipotential method leads to a single variation principle and a single inequality. From Usawa algorithm, we obtain an algorithm for solving the constitutive law based on the predictor-corrector

scheme. Classically, at each time step, all the contact forces of the system is determined iteratively by the method of successive balances which is based on an algorithm of Gauss-Seidel. Each contact force is calculated by taking provisional values of forces on the other contacts. Convergence is achieved when each force inter-particle satisfies the law of unilateral contact with dry friction. In a system composed of particles  $p$  is the maximum range of interactions that constitute the critical parameter for modeling time. Over the range of interactions is important and should test for possible interactions between the grains. SIGRAME uses the partitioning coupled with a table of connectivity [23]. This technique reduces the calculation time considerably, the number of operations no longer in  $O(p^2)$  but only in  $O(p)$ ; Therefore the hard sphere model is used to describe a binary, instantaneous, inelastic collision with friction. The key parameters of the model are 1) the coefficient of restitution ( $0 < e < 1$ ); 2) the coefficient of friction ( $\mu > 0$ ) [24].

### 2.2.2 Treatment of collisions

The collision model used in this work follows mainly the methodology proposed by [25], two parameters defining particle to particle and particle to wall interactions are introduced, first parameter is the coefficient of normal restitution; ( $e = 0.9$ ), which characterizes the incomplete restitution of the normal component of the relative velocity at the contact point and the second parameter is the coefficient of dynamic friction; ( $\mu = 0.3$ ), which arises in collisions involving sliding. In discrete particle models for each individual particle, an equation of motion is solved during the free flight phase:

$$m_i \frac{d\vec{v}_i}{dt} = m_i \vec{g} + \vec{F}_{C,i} + \vec{F}_{D,i} \quad (3)$$

Where  $m_i$ ,  $\vec{v}_i$  represent the mass and the velocity of the  $i$ th particle,  $\vec{g}$  is gravity acceleration,  $\vec{F}_{C,i}$  is the sum of contact forces (normal force and tangential force) between the particles which calculated by code SIGRAME,  $\vec{F}_{D,i}$  is the drag force is quantified through the equation:

$$F_{D,i} = C_D \pi \rho_f d_p^2 |\vec{v}_f - \vec{v}_i| \frac{(\vec{v}_f - \vec{v}_i)}{8} = C_{D,i} \pi \rho_f d_p^2 |\vec{v}_f - \vec{v}_i| \frac{(\vec{v}_f - \vec{v}_i)}{8} f(\varepsilon)^m \quad (4)$$

Where  $C_D$  is the drag coefficient,  $d_p$  is the particle diameter,  $\rho_f$  is fluid density,  $v_f$  is fluid velocity,  $\varepsilon$  is the porosity, and  $m$  is a parameter. Schiller and Naumann [26] give the drag coefficient  $C_{D,i}$  on a single sphere:

$$C_{D,i} = \begin{cases} \frac{24}{Re_p} (1 + 0.15 Re_p^{0.687}) & \text{if } Re_p < 1000 \\ 0.44 & \text{if } Re_p \geq 1000 \end{cases}$$

$$Re_p = \frac{\varepsilon \rho_f d_p |\vec{v}_f - \vec{v}_i|}{\mu_f} \quad (5)$$

$f(\varepsilon)$  is a porosity function correcting the terminal velocity or the slip velocity of a particle due to the presence of other particles (hindered settling effect) as they affect

the flow pattern in a uniform suspension [27]:

$$f(\varepsilon) = \varepsilon^{-n} \quad (6)$$

With

$$n = \frac{\log\left(\frac{Re_{mf}}{Re_t}\right)}{\log\varepsilon_{mf}} \quad (7)$$

Where  $Re_{mf}$  is the Reynolds number at minimum fluidization (drag equals the weight of the particles in the settled bed at maximum concentration,  $\varepsilon = \varepsilon_{mf}$ , i.e., minimum fluidization condition), and  $Re_t$ , the Reynolds number at terminal velocity  $v_{t,0}$ , (drag equals the weight of an isolated particle  $\varepsilon = 1$ ). The parameter  $m$  is equal to 1 for laminar interstitial flow ( $Re_p < 1$ ), 2 for turbulent interstitial flow ( $Re_p > 1000$ ) and an intermediate value in the transition regime ( $1 < Re_p < 1000$ ). Based on these [28, 29, 30] proposed a general relation for the sedimentation and fluidization for mono-dispersed spheres in laminar ( $m = 1$  and  $n = 4.7$ ), intermediate and turbulent interstitial regimes ( $m = 2$  and  $n = 2.35$ ). The function of porosity in the expression of the drag force equations (4)&(8) reduces to:

$$f(\varepsilon)^m = \varepsilon^{-m.n} \quad (8)$$

The drag function is used in this study and can be expressed:

$$C_D = C_{D,i}f(\varepsilon)^m = C_{D,i}\varepsilon^{-4.7} \quad (9)$$

### 2.2.3 Coupling DEM-CFD

DEM- CFD simulations have to cover a huge variety of regimes. The physics must be described correctly where the particle motion is controlled by the fluid flow. In this paper the type of coupling between CFD and DEM is simple. The first step is the calculation of fluid flow, done by CFD (code\_Saturne) without particles. After that, apply the results of CFD on DEM (code SIGRAME) on to calculate the drag force on each particle, and then the behavior of the fluidized bed. The long term goal is to develop a DEM-CFD solver being robust and efficient enough to handle industrial granular flow applications.

### 2.2.4 Numerical simulation for a single sphere

In order to extend the understanding of a sphere's trajectory, the flow over a stationary sphere is investigated in the turbulence regime at ( $Rep = 1000 - 10000$ ) for different sphere diameters (0.5, 1 and 2 mm). The idea is to design a box with a sphere in the center. The sides of numerical box are 24 times the diameter of sphere to prevent the effect of the walls with fluid flow in z-direction, and then calculate the drag force in 3D fluid flow over one stationary sphere fluid with different sizes, using two types of meshing (moderate and fine) in Salome and calculated by CFD (code\_Saturne) numerically. The models that used in code\_Saturne for turbulence flow are *standard*( $k - \epsilon$ )

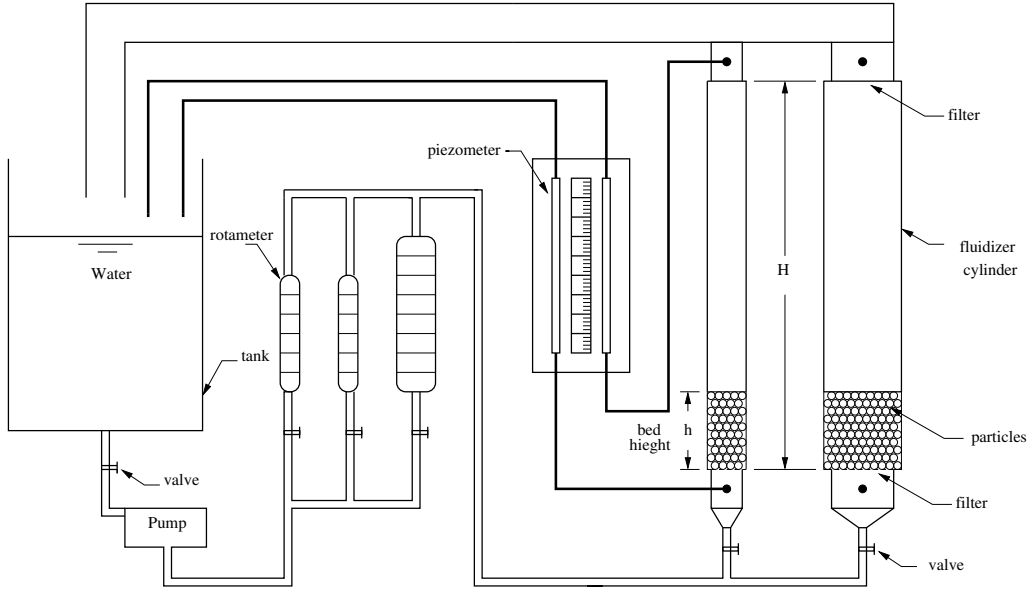


Figure 1: Schematic showing the experimental facility for fluidized bed

and  $(k - \epsilon)$  linear production ( $LP$ ) for verification of the results. The drag force ( $F_D$ ) is calculated to be the sum of pressure force and the shear stress force of the fluid flow effects on the surface of stationary sphere, therefore the drag force is increase with increase the flow rate.

### 3 Experimental procedure for Fluidized Bed

In order to show the feasibility of the DEM-CFD solver a simple experimental test is presented here. It has been found that the fluctuation and expansion ratios are the function of static bed heights, particle sizes, densities and mass velocities [31]. The experimental facility for fluidized bed as shown in figure (1) presents two cylindrical transparent columns with different internal diameters (42.3, 97 mm) respectively and the height for both of them is ( $H=1\text{m}$ ). The particles are spheres made of glass with a diameter of (2 mm) and a density of ( $2442\text{kg.m}^{-3}$ ). Gravitational acceleration of ( $9.81\text{m.s}^{-2}$ ) is acting on the particles in negative z-direction. The fluid which is used is water with dynamic viscosity ( $0.001\text{pa.s}^{-1}$ ). The initial bed height is ( $h=100\text{ mm}$ ), packed on the lower side of the cylinder, and flow rate is measured at the entrance of the column by a rotameter .

## 4 Results and Discussion

### 4.1 Numerical results of single sphere

The numerical results are presented as function of Reynolds numbers, the results shows that the values of drag force is increase with the increases of Reynolds number of the single sphere presented in figures (2,3,4).

From the results it's obvious that the value of drag force effect on the single sphere

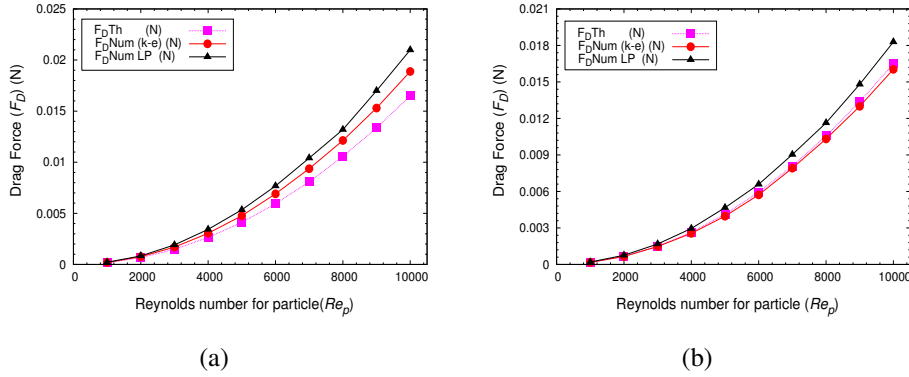


Figure 2: The Drag Force( $F_D$ )as function of Reynolds number for particle of diameter( $0.5mm$ ); ( $Re_p$ ), using two type of meshing ; a) moderate mesh and b) fine mesh

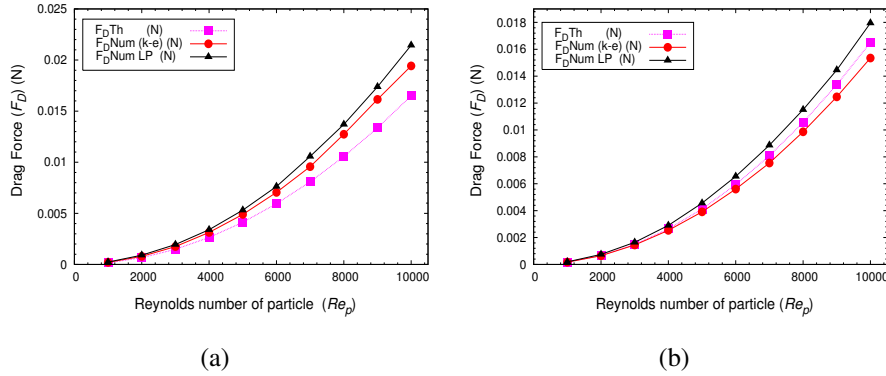


Figure 3: The Drag Force( $F_D$ )as function of Reynolds number for particle of diameter( $1mm$ ); ( $Re_p$ ), using two type of meshing ; a) moderate mesh and b) fine mesh

with different diameters depends on the type of mesh (moderate and fine) for the same values of variables and compared with the theoretical value of drag force ( $F_{DTh}$ ) that calculated from equation 4, where the values of drag force numeric of *standard*( $k-\epsilon$ ) and ( $k-\epsilon$ )*linear production*(LP) models are greater than the theoretical values of drag force for moderate mesh, but for fine mesh the numeric values of drag force



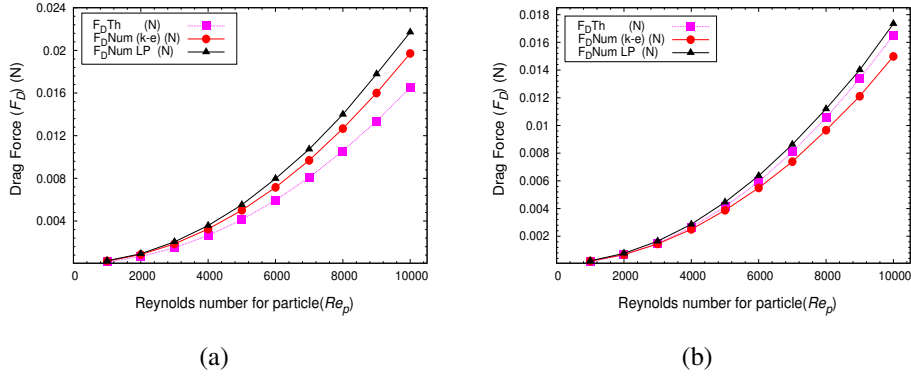


Figure 4: The Drag Force( $F_D$ ) as function of Reynolds number for particle of diameter ( $2mm$ ); ( $Re_p$ ) using two type of meshing ; a) moderate mesh and b) fine mesh

that produced by  $LP$  model are greater than theoretical and numerical values produced by  $standard(k - \epsilon)$ , thus for the three size of spheres ( $0.5, 1$  and  $2mm$ ) the values of drag force produced by  $standard(k - \epsilon)$  model approach from the theoretical value of drag force. The comparison between the two models of turbulence ( $standard(k - \epsilon)$  and  $LP$ ) is presents in figures (5,6), where the ratio between theoretical drag force and numerical drag force ( $F_{DTh}/F_{DNum}$ ) is show that for meshing type moderate the force ratio is less than 1 for two models as shown in figure (5a, b), it's meaning that the numeric values are more than the theoretic values, and for meshing type fine the ( $F_{DTh}/F_{DNum}$ ) for the three size of sphere is approach and little more than 1 for  $standard(k - \epsilon)$  model as show in figure (6a) and approach to 1 for  $LP$  model as shown in figure (6b), from figure (6a) the numeric values produced by  $standard(k - \epsilon)$  model is the nearest to the theoretic values.

Fluid flow over a stationary sphere will generate forces in x, y and z directions

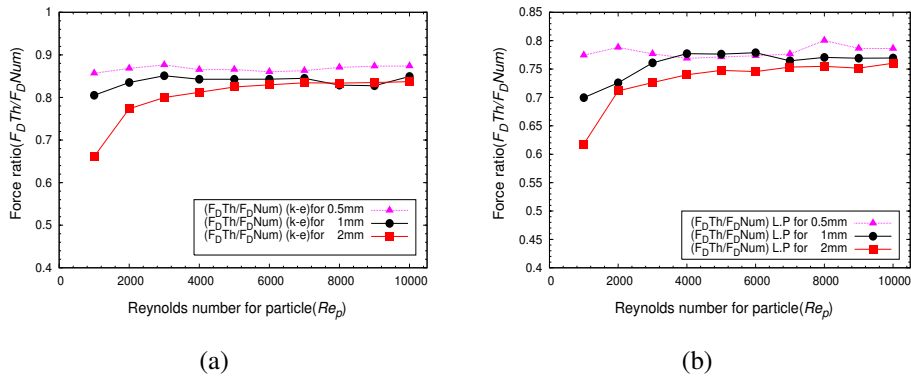


Figure 5: The force ratio( $F_{DTh}/F_{DNum}$ ) as function of Reynolds number for particle; ( $Re_p$ ), using moderate mesh ; a) for standard ( $k - \epsilon$ ) model and b) for  $LP$  model

( $F_x, F_y$  and  $F_z$ ) where ( $F_z$ ) represents the numerical drag force ( $F_{DNum}$ ) and the two other forces are produced a cause of un symmetry flow on the surface of the sphere. it's obvious that the effect of the meshing on the forces creating "parasites" that

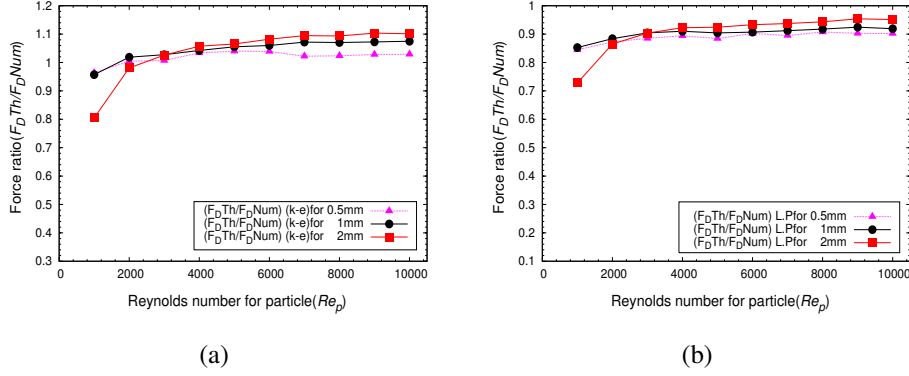


Figure 6: The force ratio( $F_DTh/F_DNum$ ) as function of Reynolds number for particle; ( $Re_p$ ), using fine mesh ; a) for standard ( $k - \epsilon$ )model and b) for  $LP$  model

diminish with the fineness of the mesh.

## 4.2 Experimental and Numerical results for fluidized bed

The most important parameter of particular interest when working with fluidized beds is the minimum fluidization velocity( $v_{mf}$ ). As fluidization proceeds the pressure drop is traced as function of increasing superficial velocity of the fluid ( $v_f$ ), and then the defluidization is obtained by decreasing the superficial velocity. The intersection between the two curves (fluidization and defluidization) is the minimum fluidization velocity( $v_{mf}$ ) as shown in figure (7a,b). The experiment shows that the ( $v_{mf}$ ) for par-

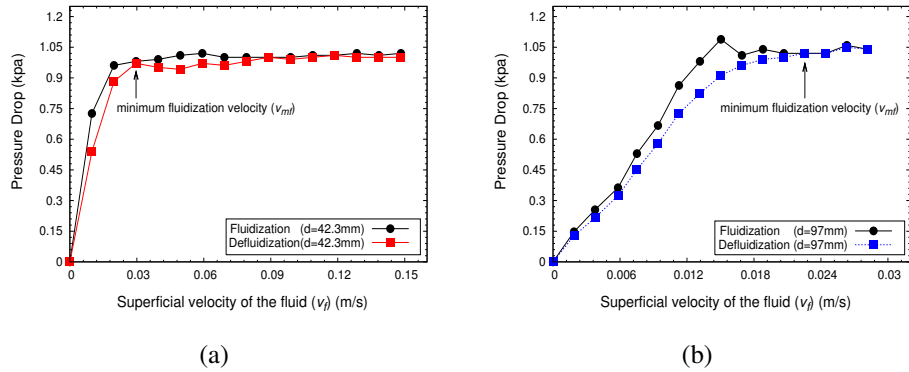


Figure 7: The Pressure Drop (kpa) as function of the Superficial velocity of the fluid; ( $v_f$ )( $m.s^{-1}$ ), a) for column diameter(42.3mm) and b) for column diameter (97mm)

ticles increase as the diameter of the fluidization column is reduced. As comparing the theoretical value of minimum fluidization velocity calculating from Kozeny-Carman equation with the experimental value; the theoretical value approaches the experimental value where, ( $v_{mf}Th = 0.02534(m.s^{-1})$ ), ( $v_{mf}Exp = 0.02966(m.s^{-1})$ ) for column (d=42.3mm) and ( $v_{mf}Th = 0.02635(m.s^{-1})$ ), ( $v_{mf}Exp = 0.02256(m.s^{-1})$ ) for

column ( $d=97\text{mm}$ ).The reasons for this little disparity between the theoretical value and the experimental value are to be seek in the experimental measurements errors, and in the fact that theoretical calculation does not take into account the column diameter influence, the bed height, and the walls effect on the particles.

The experimental and numerical results are presented in figure(8) for the case  $m.n=2.8$ ,

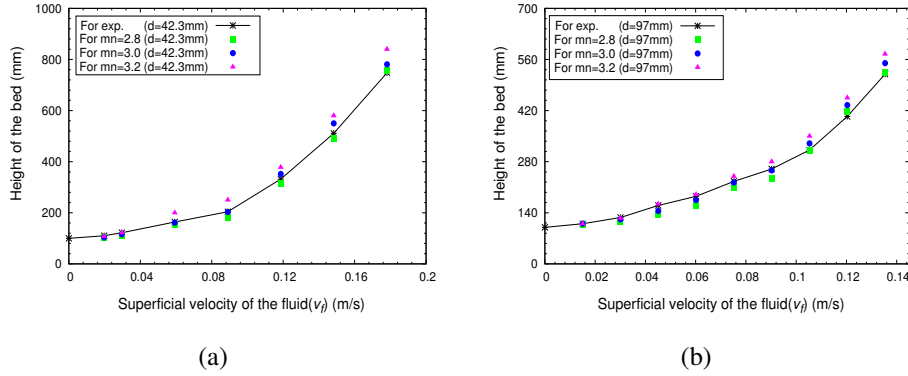


Figure 8: The height of bed as function of superficial velocity of the fluid;  $(v_f)(m.s^{-1})$ , a) for column diameter(42.3mm) and b) for column diameter (97mm)

3.0 and 3.2, for both column (42.3, 97 mm).The numerical results are identical in some points with the experimental results and with percentage of error in other points, the best parameter of  $m.n$  is between 2.8 and 3.0 from the figure (8), Anyway, comparison of experimental results with numerical values is already very promising.

## 5 Conclusion

The study presents a first step in modeling the hydrodynamic behavior of a fluidized bed by means of a coupling between a discrete element code, and a CFD calculation.For CFD, two turbulence models are compared in terms of drag force on a static sphere (*standard*( $k-\epsilon$ ) and ( $k-\epsilon$ )*Linear Production(LP)model*).The action of the fluid on the particles is expressed in terms of drag force requiring a good estimation of the local porosity. The comparison of numerical simulations with experimental results, (in two columns with different diameters) presents already a very good fit, while the coupling model is relatively simple. The perspectives of this study concern the influence of the porosity estimation on the numerical calculation, validation of the method on different geometries, and the realization of a complete coupling CFD-MED, leading to a satisfactory model for the fluidized bed and in particular of the fluid phase behaviour.

## References

- [1] A. Rao, J. S. Curtis, "The effect of column diameter and bed height on minimum fluidization velocity", *AICHE Journal*, 56, 9, 2304-2311, 2010.
- [2] P.A. Cundall, O.D.L. Strack, "A discrete numerical model for granular assemblies", *Geotechnique*, 29, 47-65, 1979.
- [3] P. Coorevits, C. Marie, K. Benhabib, "Modeling the discharge of a powder fire extinguisher by mixed discrete element method (DEM) and computational fluid dynamics (CFD)", *European Journal of Computational Mechanics*, 20, n7-8, 487-502, 2011.
- [4] P. Coorevits, C. Marie, K. Benhabib, "Mixed Discrete Element Method-Computational Fluid Dynamics Method applied to a Fire Extinguisher", in B.H.V. Topping, J.M. Adam, F.J. Pallars, R. Bru, M.L. Romero, (Editors), "Proceedings of the Seventh International Conference on Engineering Computational Technology", Civil-Comp Press, Stirlingshire, UK, Paper 134, 2010. doi:10.4203/ccp.94.134
- [5] F. P. Di Maio and A. Di Renzo, "DEM-CFD Simulations of fluidized beds with application in mixing dynamics", *KONA Journal*, 25, 205-216, Italy, (2007).
- [6] D. Gidaspow, "Multiphase flow and fluidization", Academic Press, New York, 1994.
- [7] H.P. Zhu, Z.Y. Zhou, R.Y. Yang and A.B. Yu, "Discrete particle simulation of particulate systems: Theoretical developments", *Chemical Engineering Science Journal*, 62, 3378 - 3396, 2007.
- [8] Y.Q. Feng, B.H. Xu, S.J. Zhang, A.B. Yu and P. Zulli, "Discrete particle simulation of gas fluidization of particle mixtures", *AICHE Journal*, 50, 1713-1728, 2004.
- [9] Y. Tsuji, T. Kawaguchi and T. Tanaka, "Discrete particle simulation of two-dimensional fluidized bed", *Powder Technology*, 77, 79-87, 1993.
- [10] B.P.B. Hoomans, J.A.M. Kuipers, W.J. Briels, and W.P.M. van Swaaij, "Discrete particle simulation of bubble and slug formation in a two-dimensional gas-fluidised bed: a hard-sphere approach", *Chemical Engineering Science*, 51, 99-118, 1996.
- [11] Y. Kaneko, T. Shiojima and M. Horio, "DEM simulation of fluidized beds for gas-phase olefin polymerization", *Chemical Engineering Science*, 54, 5809-5821, 1999.
- [12] M.J. Rhodes, X.S. Wang, M. Nguyen, P. Stewart and K. Liffman, "Use of discrete element method simulation in studying fluidization characteristics, influence of interparticle force", *Chemical Engineering Science*, 56, 69-76, 2001a.
- [13] B.H. Xu, A.B. Yu, "Numerical simulation of the gas-solid flow in a fluidized bed by combining discrete particle method with computational fluid dynamics", *Chemical Engineering Science*, 52, 2785-2809, 1997.
- [14] B.P.B. Hoomans, J.A.M. Kuipers and W.P.M. van Swaaij, "Granular dynamics simulation of segregation phenomena in bubbling gas-fluidised beds", *Powder Technology*, 109, 41-48, 2000.

- [15] E. Helland, R. Occelli and L. Tadrist, "Numerical study of cluster formation in a gas-particle circulating fluidized bed", *Powder Technology*, 110, 210-221, 2000.
- [16] E.K. W. Poon, G. Iaccarino, A. S. H. Ooi and M. Giacobello, "Numerical studies of high Reynolds number flow past a stationary and rotating sphere", 7th International Conference on CFD in the Minerals and Process Industries CSIRO, Melbourne, Australia, 2009.
- [17] E. Achenbach, "Experiments on the flow past spheres at very high Reynolds numbers", *Journal Fluid Mech.*, 54, 565, 1972.
- [18] S. Taneda, "Experiment Investigation of the wake behind a sphere at low Reynolds numbers", *Journal Phys.Soci.*, 11, 1104-1108, Japan, 1956.
- [19] G. Constantinescu and K. Squires, "Numerical investigation of flow over a sphere in the subcritical and supercritical regimes", *Phys. Fluids*, 16, 1449-1466, 2004.
- [20] P. Ploumhans, G.S. Winckelmans, J.K. Slamon, A. Leonard and M.S. Warren, "Vortex Methods for direct numerical simulation of three dimensional bluff body flow: Application to the sphere at  $Re = 300, 500, \text{ and } 1000$ ", *Journal Comp. Phys.*, 178, 427-463, 2002.
- [21] K. Benhabib, C. Marie, P. Coorevits, "Numerical studies of the fluidization by coupling between discrete element method (DEM) and computational fluid dynamics (CFD)", 19th International Congress of Chemical and Process Engineering CHISA2010, Prague, 2010.
- [22] J. Fortin, G. de Saxc, "Modlisation numrique des milieux granulaires par l'approche du bi-potentiel", *C. R. Acad. Sci.*, 327- srie I Ib, 721- 724, 1999.
- [23] J. Fortin, P. Coorevits, "Selecting contact particles in dynamics granular mechanics systems", *Journal of Computational and Applied Mathematics*, 168, 207-213, 2004.
- [24] J. Li and J. A. M. Kuipers, "Flow Structure formation in high-velocity gas-fluidized beds", CFB-7 at Niagara Falls, 2002.
- [25] Y. Wang, M.T. Mason, "Two-dimensional rigid-body collisions with friction", *Journal Appl. Mech.*, 59, 635, 1992.
- [26] L. Schiller, A.Z. Naumann, "A drag coefficient correlation", *Ver. Deut. Ing.*, 77, 318-320, 1935.
- [27] J.F. Richardson, W.N. Zaki, "Sedimentation and fluidization: Part 1", *Trans. Inst. Chem. Eng.*, 32, 35-53, 1954.
- [28] A.D. Maude, R.L. Whitmore, "A generalized theory of sedimentation", *Brit. Journal Appl. Phys.*, 9, 477-482, 1958.
- [29] C.Y. Wen, Y.H. Yu, "Mechanics of fluidization", *Chem. Eng. Prog. Symp. Ser.*, 62, 100-111, 1966.
- [30] E. Helland, R. Occelli, L. Tadrist, "Computational study of fluctuating motions and cluster structures in gas particle flows", *International Journal of Multiphase Flow*, 28, 199-223, 2002.
- [31] Y. K. Mohanty, G. K. Roy and K. C. Biswal, "Effect of column diameter on dynamics of gas-solid fluidized bed: A statistical approach", *Chemical Technology Journal*, 16, 17-24, India, 2007.